Green Chemistry

TUTORIAL REVIEW

View Article Online
View Journal | View Issue

Cite this: *Green Chem.*, 2016, **18**, 622

Review: nanocelluloses as versatile supports for metal nanoparticles and their applications in catalysis†

Madhu Kaushik and Audrey Moores*

Received 17th October 2015,
Accepted 4th January 2016

DOI: 10.1039/c5gc02500a

www.rsc.org/greenchem

Nanocelluloses, derived from the biopolymer cellulose, are a class of sustainable functional nanomaterials featuring exciting properties. They have been extensively researched as key components in the design of super capacitors, pH-responsive reversible flocculants, aerogels, sensors, pharmaceuticals, chiral materials and catalysts. This review will focus on the applications of nanocelluloses in catalysis. The first part illustrates their use as support, stabilizer and/or reducing agent in the synthesis of various metal nanoparticle. Subsequently, the applications of these metal-hybrid nanocellulose composites in catalysis are reviewed. Finally, catalysis involving nanocelluloses, without the use of metal nanoparticles, is reviewed.

1. Introduction

The term "nanocelluloses" broadly defines a class of nanomaterials obtained *via* top-down approaches from vegetal or bacterial cellulose. Cellulose is the most abundant biopolymer on earth and is composed of repeat units of cellobiose, a dimer of glucose where each molecule of glucose is joined by a β-1,4-glycosidic linkage (Fig. 1). In nature, these cellulose chains are assembled to form microfibrils, which are further bundled into macrofibers and fibers, in a hierarchical structure directed by hydrogen bonding.[4] Native cellulose is highly crystalline in nature and the study of this property has been the topic of intense research and debates, notably to define monocrystallites typical size within cellulose.[4] Interestingly, hydrolysis of these structures using strong acids results in the

Centre for Green Chemistry and Catalysis, Department of Chemistry, McGill University, 801 Sherbrooke St West, Montreal, QC H3A 0B8, Canada.
E-mail: audrey.moores@mcgill.ca; Fax: +1 (514) 398 3797; Tel: +1 (514) 398 4654

† In memoriam of Robert Marchessault (1928–2015), who was among the first to study the properties of cellulose nanocrystals, at McGill University over 50 years ago.[2]

Madhu Kaushik

Madhu Kaushik received her M.Sc. (H.S.) in chemistry at Panjab University, Chandigarh in 2005. Then she worked as a research chemist for a drug discovery centre, Panacea Biotec Ltd., focusing on structure-activity relationship, patentability and quality assurance. Presently, she is a finishing PhD student in the Moores research group at McGill University, Montreal, where she develops applications of cellulose nanocrystals as support for metal nanoparticles in catalysis. She has secured several awards for best posters and presentations at various conferences and currently holds a Heather Munroe-Blum Fellowship in Green Chemistry. Her research interests include nanoparticle synthesis, catalysis, sustainability and green chemistry.

Audrey Moores

Audrey Moores completed her PhD at the Ecole Polytechnique, France in 2005 with Prof. Pascal Le Floch. She was a post-doctoral fellow at Yale University in 2005–2006 under the guidance of Prof. Robert H. Crabtree. She is now an associate professor in the Department of Chemistry at McGill University and Canada Research Chair in Green Chemistry. She is also the co-associate director of the Quebec Center for Green Chemistry and Catalysis since 2012, and an associate editor for RSC Advances since 2015. In 2011, she was awarded a Science Communication Fellowship for Green Chemistry by the Environmental Health News and Advancing Green Chemistry.

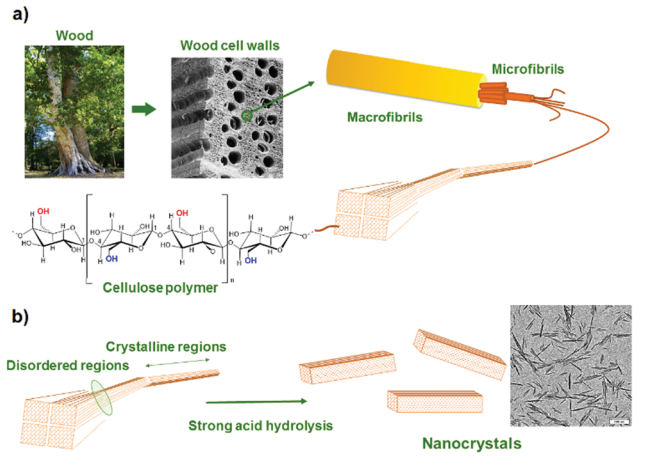

Fig. 1 (a) Structural hierarchy of the cellulose fiber component from the tree to the anhydroglucose molecule. (b) Preparation of nanocrystals by selective acid hydrolysis of cellulose microfibrils. Reproduced with permission from ref. 1.

breakage of only the most accessible glycosidic linkages within the cellulose structure, and the liberation of nano-sized and crystalline cellulose materials, also called nanocelluloses. The most common hydrolysis method relies on sulfuric acid, because it introduces a small number of sulfate ester groups on the nanocellulose surfaces, making them easily dispersible in water.[6–8] Cellulose crystallites were isolated for the first time in the late 1940s *via* this method from cotton.[10] Soon after, Rånby showed that stable colloidal suspensions of these negatively charged cellulose particles could be obtained.[11,12] Other synthetic techniques include mechanical refining, HCl or enzymatic hydrolysis, which do not affect their surface chemistry.[14]

Nanocelluloses are rod-like or ribbon-like objects with a length typically ranging from 50–1000 nm and a width varying from 3–50 nm, and therefore with high length-to-width (aspect) ratios (10 to 100).[15–19] Their morphology largely depends on the cellulose source and the conditions of preparation (type and concentration of acid, acid-to-cellulose ratio, reaction time and temperature). They have been produced from a wide variety of sources,[20] such as wood, cotton, bamboo,[21] bacteria,[22] algae, tunicates,[23] eucalyptus,[21] spruce bark,[24] soy husk,[25] *etc*. The size and morphology of nanocellulose have been well-defined and extensively studied[1,26,27] because they both influence their colloidal and macroscopic properties such as suspension rheology, phase separation concentration, liquid crystal behavior, orientation under electric or magnetic field and mechanical reinforcement ability in nanocomposites.[15,24] They have a high specific surface area,[28] high aspect ratio, high crystalline order and chirality, superior mechanical strength, and controllable surface chemistry.[16,17,29–31] In addition, they are renewable, biodegradable, non-toxic,[32–35] thermally stable and accessible industrially in large scale.[36]

In 1959, Marchessault *et al.* first demonstrated that colloidal suspensions of CNCs spontaneously organize into a chiral nematic phase above a certain critical concentration.[37] Consequently, CNCs have been used to produce iridescent and birefringent films,[38,39] for biotemplating to produce chiral mesoporous silica[40–43] and carbon,[44] titania films[45–47] and gold nanoparticle films with chiral plasmonic properties.[48,49] Their high mechanical strength have been exploited since the mid 1990's, when it was shown that CNCs were efficient reinforcing fillers in latex-based polymer matrices, leading to applications in polymer and plastic manufacturing.[16,23,50,51] More recently, they have been used for producing hydrogels,[52] aerogels,[53,54] shape memory polymers,[55] sensors,[56] and pH-responsive flocculants.[57,58] As a consequence, nanocelluloses have been applied to the paper, cosmetics, food, pharmaceuticals and biomedical industries.[59–61] Several review articles and book chapters have been published over the last years that detail the various properties and applications of nanocelluloses.[13,15–17,26,29–31,62–75]

A key feature in the development of novel catalysts resides in the importance of engineering an easy recovery step.[76] Among the many applications of nanocelluloses, their use in the design of such recyclable catalysts is appealing for a number of reasons: (1) the high surface area, thermal stability and functionalizable surface makes them interesting supports; (2) the natural surface chemistry of nanocellulose, mostly composed of hydroxy and sulfate ester groups, play a key role in their ability to reduce metal species, and their high crystalline order and chiral properties may participate in catalytic events; (3) nanocellulose suspensions in water are very stable and confer enhanced stability to catalysts supported by them. They afford avenues for the generation of biphasic catalytic systems akin to, for instance, ionic liquids;[77,78] (4) finally nanocelluloses are bio-sourced, biodegradable, non-toxic, and available industrially in large scale. The most developed approach has been to use nanocelluloses as support for metal nanoparticles (NPs). Other examples include the grafting of organometallic species or the chemical modification of the nanocelluloses to afford organocatalysts. In the following sections, we introduce the nanocelluloses nomenclature and their various properties. Then we detail how nanocelluloses are used to produce supported metal NPs and review the use of these hybrid systems in catalysis. At last, other applications of nanocelluloses in catalysis in absence of metal NPs are covered.

2. Nanocellulose nomenclature

In the literature, a wide range of nomenclature is used to categorize these nanocelluloses, for example, nanocrystallites of cellulose (NCCs), nanocrystalline cellulose (NCCs), cellulose nanocrystals (CNCs), cellulose nanowhiskers (CNWs), cellulose nanofibers (CNFs), nanofibrillated cellulose (NFCs), nanofibrous cellulose (NFCs), bacteria cellulose, bacterial cellulose and/or bacterial nanocellulose (BCNs). In the past, attempts have been made to rationalize the use of these terms based on their morphology and synthetic procedure.[15,17,26,72,75] We have summarized the nomenclature of nanocelluloses in Table 1 based on their size distribution and method of preparation.

Table 1 Nomenclature and size distribution of nanocelluloses

Nomenclature	Abbreviations	Size distribution (nm)	Mode of preparation (sources)	Ref.[a]
Cellulose nanocrystals, nanocrystalline cellulose, nanocrystallites of cellulose, crystalline cellulose, cellulose nanowhiskers	CNCs, NCCs, CNXLs, XNLs, CNWs	Length: 50–500 Width: 3–15	Acid hydrolysis (wood, cotton, rice, ramie, sisal, tunicates)	14,80–88
Cellulose nanofibers, nanofibrillated cellulose, nanofibrous cellulose	CNFs, NFCs	Length: 50–3000 Width: 5–50	Mechanical treatment (wood, microcrystalline cellulose, tunicates)	14,80,81,89–94
Bacteria cellulose, bacterial cellulose, bacterial nanocellulose, bacteria nanofiber	Bacteria CNs, BNCs, BNFs	Length: 200–3000 Width: 10–75	Bacteria	14,95–97

[a] Proposed references are representative examples and do not constitute an exhaustive list.

We have broadly categorized the nanocelluloses into three categories in Table 1: (i) nanocrystallites of cellulose (NCCs), nanocrystalline cellulose (NCCs), cellulose nanocrystals (CNCs) and/or cellulose nanowhiskers (CNWs), which are produced from acid hydrolysis and are typically shorter in length, narrower in width and higher in crystallinity; (ii) cellulose nanofibers (CNFs), nanofibrillated cellulose (NFCs) and/or nanofibrous cellulose (NFCs), which are those obtained from mechanical treatment and are frequently longer, wider and lower in crystallinity, and (iii) bacterial cellulose and/or bacterial nanocellulose (BCNs), which are derived from bacteria, and are the longest and widest in the family. It is essential to introduce a standard nomenclature for the family of nanocelluloses. Some attempts in this directions have been taken by the Technical Association of Pulp and Paper Industries (TAPPI).[79] However, there is no set definition for each sub-set yet, and the literature reveals that various nanocelluloses coexist in the broad and overlapping material space. In our review, the applications of all forms of nanocelluloses in catalysis shall be included.

3. Nanocelluloses as support for metal NPs

Applications of nanocelluloses as a metal NP support has attracted a lot of attention in the past decade. Metal NPs possess properties which are unique and distinct from those of their bulk or molecular counterparts.[98] Metal NPs are thermodynamically unstable and tend to aggregate to form bulk metal without the use of capping agents, ligands or supports in their synthesis. Because of their high surface area, reductive surface functional groups and water suspendability, nanocelluloses are attractive supports for metal NPs. The following section shall review the synthesis of metal NPs supported onto nanocelluloses in detail. Table 2 gives a list of metal NP-nanocellulose hybrid composites with non-catalytic applications, whereas Table 3 lists metal NP-nanocellulose hybrid composites with applications in catalysis.

3.1. Synthesis of metal NPs

Nanocelluloses were first used as template for synthesizing metal NPs in 2003, when Woodward and coll. precipitated Pd, Au and Ag from their metal precursors onto bacterial CNFs, without the use of any external reducing agent.[125] The next example in literature came in 2007 with the synthesis of Se and Ni NPs by Exarhos and coll.[121,122] Ni NPs of 5 to 12 nm on carbon were prepared by the thermal treatment (400–500 °C) of $Ni(NO_3)_2$ in the presence of CNCs acting as the source of carbon. Thermal reduction of CNC at lower temperatures with Se precursors was used in the synthesis of Se NPs onto rod-like carbon structures. Following these preliminary works, the use of nanocelluloses for metal NPs gradually increased. There are mainly three approaches in the synthesis of metal NPs, shown in Fig. 2 and described in the following sub-sections.

3.1.1. Reduction using an external reducing agent. The first and most common approach is to use an external reducing agent to reduce a metal precursor into metal NP on the nanocellulose surface. Ag NPs have been synthesized on various types of nanocelluloses by reducing $AgNO_3$ with $NaBH_4$.[100–102,104,106,107,109–111,126,127] Laine and coll. studied the effect of the number of sulfate ester on the CNC surface on NP formation and nucleation of Ag NPs by borohydride reduction. CNCs, with a minimum quantity of sulfate, proved to be vital for the nucleation of small, monodisperse Ag NPs.[101] Other external reducing agents like triethanolamine, NH_2NH_2, NH_4OH and ascorbic acid have also been used for reducing Ag salts into Ag NP.[110,111] Au NPs have been synthesized from $HAuCl_4$ onto nanocelluloses by using external reducing agents ($NaBH_4$[9,117,128–130] and poly(ethyleneimine[131,132]) as well. Schlesinger *et al.* demonstrated that the size of Au NPs increases with increasing concentration of the metal salt solution.[128] Borohydride reduction has also been applied towards synthesizing Pd NPs,[133] Ru NPs,[127] CuO[134] NPs, and alloy NPs, including Au–Pd,[135] Pd–Cu,[136] and Au–Ag.[115] In case of alloy NPs, varied size distributions could be achieved by varying the ratio of the two metal precursor used. A more atom-economical alternative to borohydride

Table 2 Metal, alloy and oxide NPs – nanocellulose hybrid composites with non-catalytic applications. Metal, alloys and oxides are listed in alphabetical order

Metal/oxide NP (size in nm)	Precursor (synthesis of NPs)	Nanocellulose used	Application	Ref.
(a) Silver nanoparticles				
Ag NPs (~7)	$AgNO_3$ (reduction with dopamine hydrochloride)	Polydopamine coated CNCs	Antibacterial activity	99
Ag NPs (10–80)	$AgNO_3$ (reduction by $NaBH_4$)	Amine grafted CNCs	—	100
Ag NPs (2–3)	$AgNO_3$ (reduction by $NaBH_4$)	CNCs with varied sulfur content	—	101
Ag NPs (6.3 ± 3.1)	$AgNO_3$ (reduction by $NaBH_4$)	TEMPO-oxidised CNFs	Antibacterial activity	102
Ag NPs (spherical: 1–10; dendritic: 5–10 μm)	$AgNO_3$ (reduction by CNCs: 100 °C, 12 h)	CNCs	Antibacterial activity	103
Ag NPs (3–4)	$AgNO_3$ (reduction by CNFs)	TEMPO-oxidised CNFs	Aerogels	54
Ag NPs (5–14)	$AgNO_3$ (reduction by $NaBH_4$)	Bacteria CNFs	Antibacterial activity	104
Ag NPs (17.1 ± 5.9)	$AgNO_3$ (reduction by bacterial CNFs: 80 °C, 4 h)	Bacteria CNFs	Antibacterial activity	105
Ag NPs (10–15)	$AgNO_3$ (reduction by $NaBH_4$)	TEMPO-oxidised CNCs	Antibacterial activity	106
Ag NPs (<10)	$AgNO_3$ (reduction by $NaBH_4$)	TEMPO-oxidised CNCs	DNA biosensor	107
Ag NPs (20–45)	$AgNO_3$ (reduction by aldehyde groups on CNC surface)	Periodate-oxidised surface CNCs	Antibacterial activity	108
Ag nanoclusters (size not reported)	$AgNO_3$ (reduction by $NaBH_4$)	CNFs (polymethacrylic acid (PMAA) used as stabiliser)	Antibacterial activity	109
Ag NPs (8–15)	$AgNO_3$ (reduction by triethanolamine)	Bacteria CNFs (triethanolamine as complexing agent)	Antibacterial activity	110
Ag NPs (~30)	$AgNO_3$ (reduction by NH_2NH_2, NH_2OH, ascorbic acid)	Bacteria CNFs (polyvinylpyrrolidone (PVP) and gelatin used as additional stabilisers)	Antibacterial activity	111
Ag NPs (10–20)	$AgNO_3$ (reduction by CNFs: 100 °C, 1 h)	TEMPO-oxidised bacteria CNFs	—	112
Ag NPs (size not reported)	$AgNO_3$ (reduction by sodium citrate)	Bacteria CNFs (sodium citrate as additional stabiliser)	Substrate enhanced raman scattering (SERS) substrates	113
(b) Silver salts and silver alloy nanoparticles				
AgCl NPs (size not reported)	$AgNO_3$ and NaCl	Bacteria CNFs	Antibacterial activity	114
Ag–Au alloy NPs (3–7)	$AgNO_3$ and $HAuCl_4$ ($NaBH_4$ reduction)	CNCs (capping agent used: sodium citrate)	—	115
Ag–ZnO NPs (9–35)	$AgNO_3$ and $Zn(AcO)_2{\cdot}2H_2O$ (80–100 °C, 1–2 h, pH10)	CNCs	Antibacterial activity	116
(c) Other metal, metal alloys and metal oxide nanoparticles				
Au NPs (~10)	$HAuCl_4$ (reduction by citrate ions and surface of CNFs)	Wood or bacteria CNFs	Security paper making: optical properties	117
CdS NPs (~8)	$Cd(NO_3)_2{\cdot}5H_2O$ and Na_2S	Bacterial CNFs	—	118
$Cu_{0.5}Co_{0.5}Fe_2O_4$ NPs (13.5)	$FeCl_3$, $CoCl_2$, $CuCl_2$ (200 °C, 24 h)	CNCs	—	119
Fe_3O_4 (5.9–14.1)	$FeSO_4{\cdot}7H_2O$ (reaction in NaOH)	CNCs (PDDA, PVP, SiO_2 and β-cyclodextrins used as additional stabilisers)	Adsorption of pharmaceutical residues	120
Ni NPs (5–12)	$Ni(NO_3)_2$ (reduction by CNCs: 400–500 °C, 2 h)	CNCs	—	121
Pt NPs (5–30)	H_2PtCl_6 (CNCs as reducers in $scCO_2$)	CNCs	—	5
Se NPs (10–20)	H_2SeO_3 and Na_2SeO_3 (reduction by CNCs: 100–160 °C, 16 h)	CNCs	—	122
TiO_2 NPs (length: 26 ± 3; width: 16 ± 2)	Commercial TiO_2 NPs	CNFs	—	123
TiO_2 NPs (20–60 nm aggregates)	Commercial TiO_2 NPs	CNFs	Adsorption and demetallation of heme proteins *via* electrochemistry	124

reduction is the use of H_2 gas as a reducer of metal precursors. Our group applied this approach to synthesize Pd NPs[3,137] and Ru NPs[138] onto CNCs. Notably, in the latter, CNCs not only act as supports for NPs but also participate in the reduction of Ru(III) to Ru(0). It is the first reported study where the $RuCl_3$ could be reduced to Ru(0) NPs without using strong reducing agents like $NaBH_4$, which shows the positive role of CNC in the sustainable synthesis of metal NPs. CNCs are believed to act in synergy with H_2 to perform the reduction under mild conditions of room temperature and 4 bars H_2.

Table 3 Metal/oxide NP – nanocellulose hybrid composites with catalytic applications. Metal, alloys and oxides are listed in alphabetical order

Metal/oxide NP (size in nm)	Precursor (synthesis of NPs)	Type of nanocellulose used (additional capping agent or support used, if any)	Catalytic reaction	Ref.
(a) Silver nanoparticles				
Ag NP (1.3 ± 0.3)	Ag wire and $AgNO_3$ (reduction by CNCs)	CNCs	Hydrogenation of aldehydes, 4-nitrophenol, alkenes and alkynes	149
Ag NP (~10)	$AgNO_3$ (reduction by dopamine)	Polydopamine-coated CNCs (β-cyclodextrin agent used as additional capping agent)	Reduction of 4-nitrophenol	139
Ag NPs (~6.2)	$AgNO_3$ (reduction by $NaBH_4$)	NFCs (poly(amidoamine), PAMAM, dendrimer)	Reduction of rhodamine B (decoloration of the dye)	126
Ag NPs (4.0 ± 2.0)	$AgNO_3$ (reduction by $NaBH_4$)	TEMPO-oxidised CNFs	Aza-Michael reaction	127
Ag NPs (10 to 50)	$AgNO_3$ (reduction by CNC)	CNCs	Electrocatalysis: reduction of oxygen	142
(b) Gold and gold-alloy nanoparticles				
Au NPs (4.5 ± 0.4, 5.6 ± 0.6, 7.1 ± 0.6)	$HAuCl_4$ (reduction by $NaBH_4$)	CNCs modified into mesoporous photonic cellulose by co-templating with urea/formaldehyde resin	Biosensor (undergo color changes on exposure to 2-mercaptoethanol)	128
Au NPs (2–4)	$HAuCl_4$ (reduction with and without $NaBH_4$)	PAMAM dendrimer-grafted CNCs	Reduction of 4-nitrophenol	140
Au NPs (30.5 ± 13.4)	$HAuCl_4$ (reduction by CNCs)	CNCs	Reduction of 4-nitrophenol	143
Au NPs (2–3)	$HAuCl_4$ (reduction by -HS groups on the CNC surface)	HS-functionalized CNC	Alkyne–aldehyde–amine-coupling	141
Au NPs (2.95 ± 0.06)	$HAuCl_4$ (reduction by $NaBH_4$)	Poly(diallyldimethyl ammonium chloride) (PDDA)-coated carboxylated CNCs	Reduction of 4-nitrophenol	9
Au NPs (~9)	$HAuCl_4$ (reduction by poly(ethyleneimine)	Bacteria CNFs (heme proteins: horseradish peroxidase, hemoglobin and myoglobin immobilised onto CNFs)	Electrocatalysis: reduction of H_2O_2	150
Au NPs (~9)	$HAuCl_4$ (reduction by poly(ethyleneimine)	Bacteria CNFs: poly(ethyleneimine) used as linking agent	Electrocatalysis: reduction of H_2O_2 in biosensers	131
Au NPs (<5)	$HAuCl_4$ (reduction by $NaBH_4$)	CNFs	Reduction of 4-nitrophenol	130
Au NPs (2–7)	$HAuCl_4$ (reduction by $NaBH_4$)	TEMPO-oxidised CNFs	Enzyme immobilisation: bio-catalysis	151
Au–Pd NPs (4–9)	$HAuCl_4{\cdot}3H_2O$ and $[Pd(NH_3)_4]{\cdot}Cl_2$ (reduction by $NaBH_4$)	TEMPO-oxidised CNFs	Reduction of 4-nitrophenol	135
(c) Cadmium sulphide nanoparticles				
CdS NPs (10–20)	$CdCl_2$ (thermal treatment in presence of thiourea)	Bacteria CNFs	Photocatalysis: methyl orange (MO) degradation	152
(d) Copper, copper oxide and copper alloys nanoparticles				
Cu NPs (~5)	$CuCl_2$ (reduction by ascorbic acid)	TEMPO-oxidised CNFs	Reduction of 4-nitrophenol	153
CuO NPs (~7)	$CuSO_4$ (reduction by $NaBH_4$)	CNCs	Reduction of 4-nitrophenol	134
Cu–Pd NPs (Pd = ~3.7; Cu = ~4.0)	$PdCl_2$ and $CuCl_2$ (reduction by KBH_4)	Bacteria CNFs	Water denitrification: nitrate reduction	136
(e) Iron nanoparticles				
Fe NPs	$FeCl_3$ (Reduction by H_2)	CNCs from bamboo pulp	Methylene blue degradation, Reduction of 4-nitrophenol	148
(f) Palladium nanoparticles				
Pd NPs (1–7)	$PdCl_2$ (reduction by CNCs)	CNCs	Reduction of methylene blue and 4-nitrophenol	144
Pd NPs (~20)	$PdCl_2$ (reduction by KBH_4)	Bacteria CNFs	Heck reaction	133
Pd NPs (3.6 ± 0.8)	$PdCl_2$ (reduction by H_2)	CNCs	Hydrogenation of phenol; Heck coupling	3
(g) Platinum nanoparticles				
Pt NPs (11–101)	H_2PtCl_6 (reduction by wood nanomaterial)	Wood nanomaterials	Reduction of 4-nitrophenol	146
Pt NPs (~2)	H_2PtCl_6 (reduction by CNCs)	CNCs; carbon black as additional support	Electrocatalyst for oxygen electroreduction	147
Pt NPs (3–4)	H_2PtCl_6 (reduction by $NaBH_4$ and HCHO)	Bacteria CNFs	Electrocatalysis: oxidation of hydrogen in fuel cells	154
(h) Ruthenium nanoparticles				
Ru NPs (8.0 ± 2.0)	$RuCl_3$ (reduction by $NaBH_4$)	TEMPO-oxidised CNFs	Aerobic oxidation of benzyl alcohol	127
(i) Titania nanoparticles				
TiO_2 NP (4.3–8.5)	$Ti(OBu)_4$ (thermal treatment)	Bacteria CNFs	Photocatalysis: methyl orange degradation	155

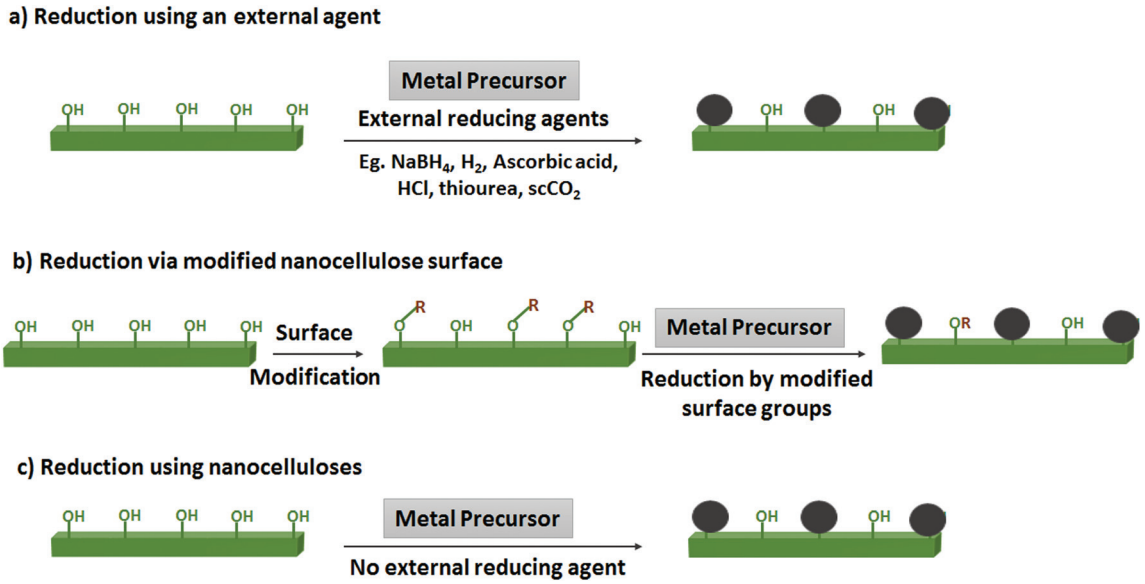

Fig. 2 Three approaches for synthesis of metal NP-nanocellulose hybrid composite: (a) reduction using an external agent, (b) reduction *via* modified nanocellulose surface, and (c) reduction using nanocelluloses.

3.1.2. Reduction *via* modified nanocellulose surface. The second approach for using nanocellulose as bio-templates for metal NPs is to modify their surface by attaching chemical groups that have reducing/coordinating capabilities, and using these modified nanocelluloses to form metal NPs from their corresponding salts, without the use of any external reducing agent. Tam and coll. used polydopamine-coated CNCs to generate Ag NPs from $AgNO_3$, where the Ag ions were reduced by dopamine.[99,139] Interestingly, they used β-cyclodextrin as an additional capping agent in one synthesis and only polydopamine-coated CNCs in the other.[139] Periodate-oxidised CNCs have also been used in the formation of Ag NPs from Ag(I) salt, where the aldehyde groups on the CNC surface have been proposed to act as reducing agents.[108] Au NPs have also been synthesized from their metal salt using surface-modified nanocelluloses as reductants. Tam and coll. grafted PAMAM (poly(amidoamine)-dendrimer onto CNCs, and the amine groups were used for reducing $HAuCl_4$ into Au NPs.[140] The size distributions of Au NPs were broader when using CNC-PAMAM as a reducing agent compared to conventional borohydride reduction, and the greater the PAMAM loading was, the more polydisperse the resulting Au NPs were. It was rationalized that PAMAM was a very active reducing agent, thus causing rapid $HAuCl_4$ reduction, excessive seeding and poor growth control. Huang *et al.* used the HS-functionalized CNCs for reducing $HAuCl_4$ to Au NPs.[141]

3.1.3. Reduction using nanocelluloses. The third approach, and the simplest, is to use the surface hydroxyl groups on the nanocelluloses itself for reducing metal precursors into metal NPs. In this method, the nanocelluloses act as both support and reducers for the generation of NPs. Through this approach, Ag NPs,[54,103,112,142] AgCl NPs,[114] Au NPs,[143] Pd NPs,[144,145] Pt NPs,[5,146,147] $Cu_{0.5}Co_{0.5}Fe_2O_4$ NPs,[119] Fe_3O_4 NPs,[120] Se NPs,[122] Ni NPs[121] and Fe[148] NPs have been synthesized *via* hydrothermal procedures. Remarkably, Thielemans, Walsh and coll. synthesized Pd NPs supported onto CNCs in a one-pot synthesis in sub-critical and supercritical CO_2 from Pd(hexafluoroacetylacetonate)$_2$ (Pd(hfac)$_2$).[145] The advantage of using supercritical CO_2 was that at the end of the reaction, dry Pd NPs supported onto CNCs were obtained simply by venting out the CO_2. Pressure (240–2200 psi), reaction time (2–17 h), and weight ratio of the precursor Pd(hfac)$_2$ to CNCs (1–4% w/w) affected the size of the Pd NPs obtained. These results show that the diameter of Pd NPs varied between 6 and 13 nm. The smaller NPs were attached on the CNCs, while NPs with diameters above 13 nm appeared not to remain attached to the CNC surface. In another work, Thielemans, Walsh and coll. synthesized Pt NPs supported onto CNCs in supercritical CO_2/water system, where they reduced H_2PtCl_6 into Pt in aqueous solution using CNCs as reducing agent. Interestingly, they reported that the reaction only proceeded when water was in contact with supercritical CO_2.[5] Recently, our group described a highly atom economical synthesis of Ag NPs onto the CNCs directly from bulk Ag metal in presence of light, water and CNC suspension. In this study, CNCs played a key role as high surface support and *in situ* reducers to drive the depletion of Ag from a metal wire and afford 1.3 nm ± 0.3 nm Ag NPs.

The mechanism of binding metal NPs onto nanocelluloses have not been studied in much detail. Unmodified nanocelluloses have a hydrophilic surface covered with hydroxyl groups. The most classically used nanocellulose rely on a sulfuric acid digestion, which also leaves sulfate esters, at the surface. When the surface is fully oxidized using TEMPO, carboxylate functionalities are introduced. All these oxygen containing

moieties are very effective metal center stabilizers *via* the formation of dative bonds.[134,143,144,146] Thiols being known for their strong affinity for metal surfaces, especially for gold, SH-functionalized CNCs were used to effectively stabilize Au NPs.[141] Interestingly, CNCs are very efficient towards the formation of small metal NPs and their stabilization, notably under catalytic conditions.[137,138]

3.2. Characterization of metal NP-nanocellulose hybrid composites

Visualization of metal NP-nanocellulose hybrid composites is an essential part of the synthesis of metal NPs onto nanocellulose surfaces. Transmission electron microscopy (TEM), cryo-TEM, atomic force microscopy (AFM), and field emission gun scanning electron microscopy (FEG-SEM) are a few visualization techniques. The most widely used technique is TEM, along with its analytical tools. TEM observation of hybrid organic–inorganic systems is very difficult because nanocelluloses and metal NPs have different density and sensitivity to beam damage.[1,27] While metallic NPs are very stable, nanocelluloses may be damaged by the electron beam, resulting in local sample destruction. Moreover, a large defocus has to be applied to visualize the less dense cellulose. When metal NPs are imaged simultaneously with nanocelluloses, this leads to an overestimation of their size. Consequently, only a few TEM images are available in the literature where nanocelluloses and supported metal NPs could be seen simultaneously with clarity.[1] To overcome this issue, negative staining with heavy metal, such as uranyl acetate, has been applied, which outlines the CNCs with precision. However, this technique is not adapted in cases where the metal NPs are smaller than 3–4 nm, a size comparable to the footprint of the halo caused by staining. Recent results demonstrated that highly sensitive direct detection device (DDD) cameras associated with phase plates allowed simultaneous observation of CNCs and sub-nanometer thick Pd patches at their surface. In this experiment, the organic and inorganic phases were observed together at near-focus conditions.[137] Representative examples of TEM images of metal NP-nanocellulose hybrid composites are displayed in Fig. 3.

Alongside visualization of metal NPs, it is very important to validate the chemical nature of the NPs seen in the images. This analysis can be done *via* TEM by using energy dispersive X-ray spectroscopy (EDX), which allows for quantitative measurement of chemical composition. Furthermore, it is vital to evaluate the oxidation state of the metal NPs, especially in the context of catalysis. For this, the most common technique used is X-ray photoelectron spectroscopic (XPS) analysis. In addition, thermogravimetric analysis (TGA) is done to monitor the thermal stability of these hybrid composites. Usually, the thermal stability of the modified nanocelluloses composites are higher than nanocelluloses alone.[156] Furthermore, X-ray powder diffraction (XRD) experiments are carried out to determine any change in crystallinity within the nanocelluloses after the modification. Usually no significant change in the crystallinity of the nanocelluloses is observed.[139] Inductive coupled plasma (ICP) coupled with atomic emission spectroscopy (AES) or mass spectroscopy (MS) as detection methods is also conducted to determine the metal loading within the synthesized hybrid materials. The same methods are also used to study the leaching of metal NPs in catalytic product, which is essential for determining the robustness and heterogeneous nature of the catalytic system.[133,134,138,149,157]

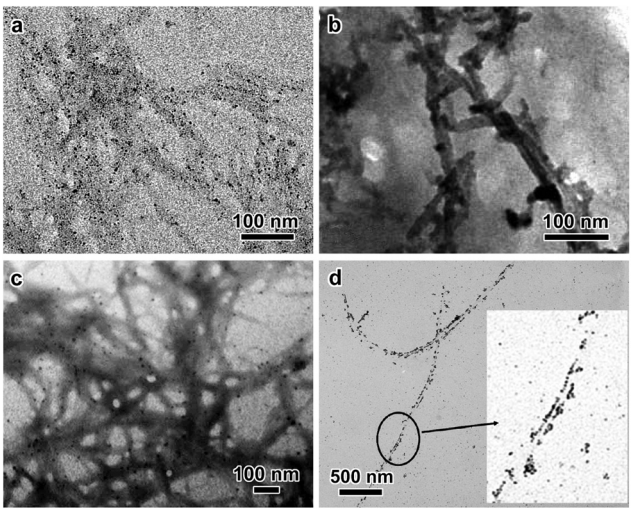

Fig. 3 TEM images of metal NPs supported by CNCs: (a) Pd on wood pulp CNCs (reproduced from Cirtiu *et al.*[3] by permission of The Royal Society of Chemistry); (b) Pt on cotton CNCs (reproduced from Benaissi *et al.*[5] by permission of The Royal Society of Chemistry); (c) Au on wood pulp CNCs (reproduced from Lam *et al.*[9] by permission of The Royal Society of Chemistry); (d) Cu on tunicate CNCs (reprinted with permission from Padalkar *et al.*[13] Copyright 2010 American Chemical Society).

4. Catalysis by metal NP-nanocellulose hybrid composites

NP catalysis has gained momentum in the recent years as they provide a bridge between the homogeneous and heterogeneous catalytic systems.[158] They combine the efficacy, selectivity, and moderate reaction conditions of homogeneous systems to the easy separation, recyclability and affordability of heterogeneous systems. Metal NP-nanocellulose hybrid composites have been more and more applied towards catalysis, especially in the last 5 years. Nanocelluloses provides interesting properties compared to conventional supports and thus afford novel catalytic systems, with unique features, notably in terms of NP stability, NP reactivity and selectivity (*vide infra*), but also with the goal of afford sustainable alternatives to known methods. Besides catalysis, they have been used for antibacterial applications,[99,102–106,108–111,114,116,154] aerogels,[54] DNA biosensors,[107] protein adsorption,[124] substrate enhanced raman scattering (SERS) substrates,[113] security paper making: optical properties,[117] and adsorption of pharmaceutical resi-

dues (Table 2).[120] In the following sections, we shall focus on the catalytic applications of the metal NP-nanocellulose hybrid composites, which have been summarized in Table 3.

4.1. Reductions

Metal NP-nanocellulose hybrid composites have been widely applied towards the reduction of 4-nitrophenol to 4-aminophenol (Scheme 1a). This reaction has been successful using Au NPs,[9,130,140,143] Ag NPs,[139] Pd NPs,[144] Au–Pd NPs,[135] Pt NPs,[146] Cu NPs[153] and CuO NPs.[134] This reduction reaction with metal NPs supported onto nanocelluloses in the presence of $NaBH_4$ occurs at room temperature, reaching completion between 15–30 min, and giving excellent conversions of 95–100%. The turn over frequencies (TOFs) for the reduction of 4-nitrophenol to 4-aminophenol by metal NPs supported onto nanocelluloses were much higher than metal NPs supported onto other polymer supports. The higher TOFs were because of the highly dispersed metal NPs, which were exposed on the nanocellulose surface, allowing effective contact with the reactants.[9,130,134,140,143] 4-Nitrophenol reduction has been postulated to follow the Langmuir-Hinshelwood mechanism. Metal hydrides are formed when borohydride ions react with metal NPs on the metal surface, with the simultaneous adsorption of nitrophenolate ions. The rate-determining step is the electron transfer from the borohydride ion to the 4-nitrophenolate ion, through the metal NP surface. This reduces the 4-nitrophenolate ion into a 4-aminophenolate ion. Finally, H^+ and 4-aminophenolate ions rearrange and 4-aminophenol desorbs from the metal surface.[9] Tam and coll. carried out the reduction of 4-nitrophenol with Ag NPs supported onto poly(dopamine)-coated CNCs. They compared the efficiency of 4-nitrophenol reduction with Ag NPs to Au, Pd and Cu NPs and found that Ag NPs featured higher TOFs compared to others. Interestingly, they could further accelerate the catalytic process with further incorporation of β-cyclodextrin into the system thanks to host–guest interactions between 4-nitrophenol and cyclodextrins. Huang and coll. inferred that the catalytic activity for the reduction of 4-nitrophenol depends on the metal NP size, that is, smaller Pt NPs exhibited enhanced catalytic activities.[146] They used varied sizes of Pt NPs for the reaction and the catalytic activities of the Pt particles followed the following order: spherical Pt NPs (2.3 ± 0.5 nm) > spherical Pt nanoclusters (21.5 ± 5.2 nm) > Pt NPs (4.5 ± 0.8 nm) > cubic Pt NPs (15.9 ± 2.9 nm). Even though the size of spherical Pt nanoclusters was larger than that of the cubic Pt NPs, the kinetic data indicated that the Pt clusters were catalytically more active than the cubic Pt NPs. This could be explained on the following account: the nanoclusters were composed of more than 50 particles with an average diameter of about 3.0 nm; the larger percentage of edge and corner atoms in structures might have increased their catalytic activities. Recently our group showed that Ag NPs supported onto CNCs could perform the same reaction but with H_2 (40 bar) as a reducer in place of $NaBH_4$, thus affording a more atom economical access to the highly demanded aromatic amines.[149]

Ramaraju *et al.* studied the decoloration of rhodamine B dye by Ag NPs supported onto CNFs, additionally stabilized by PAMAM dendrimer. The dye was reduced by $NaBH_4$ in the presence of Ag NPs acting as catalysts.[126] They explained the catalytic mechanism as follows: the nucleophilic borohydride ion donates its electrons to Ag NPs and the electrophillic Rhodamine B captures electrons from the Ag NPs. Therefore, Ag NPs serve as a catalytic electron relay for the redox

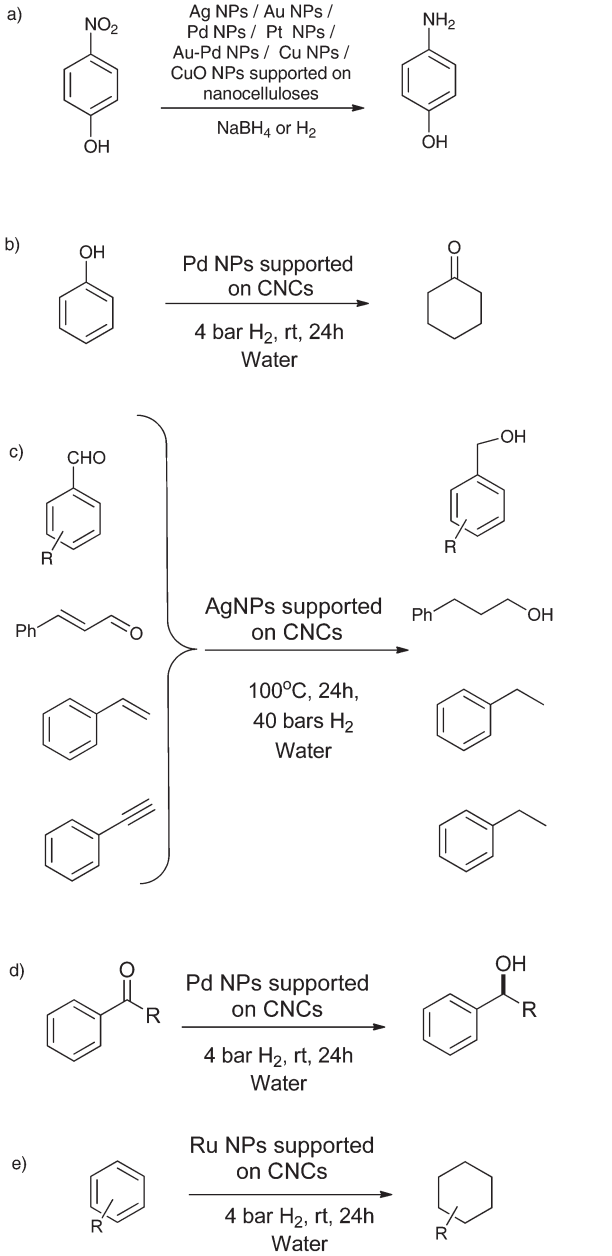

Scheme 1 Reduction reactions by metal NP-nanocellulose hybrid composites: (a) reduction of 4-nitrophenol, (b) hydrogenation of phenol, (c) hydrogenation aromatic aldehydes, alkene and alkynes, (d) enantioselective hydrogenations of prochiral ketones, and (e) arene hydrogenations.

reduction degradation of Rhodamine B. Without metal NPs, there is no electron transition. The similar reduction of methylene blue with $NaBH_4$ was reported with Pd[144] and very recently with less toxic and earth-abundant Fe[148] on nanocellulose. Interestingly, the latter example shows the use of CNC for potential water pollution remediation systems. The reduction of nitrates for water denitrification was also reported with Cu–Pd NPs on bacterial CNFs.[136]

The hydrogenation of C–C and C–O multiple bonds is a very active research field, with applications in all chemical industries, from petro chemistry to pharma, and nanocellulose hybrids afforded interesting catalytic systems for this reaction (Scheme 1).[159] Pd NPs supported onto CNCs were first described by us for the hydrogenation of phenol at 4 bars H_2, room temperature, in water for 2 h (Scheme 1b).[3] In this work, we compared the activity of PdNPs@CNCs with the one of commercial Pd catalysts on various support, such as PdNPs@Al_2O_3 and PdNPs@C, at several Pd loadings. 0.5% PdNPs@CNCs performed similarly to 1% PdNPs@Al_2O_3, which showed 100% conversion. Other commercial systems with higher loading (5% PdNPs@Al_2O_3 and 5% PdNPs@C) performed poorly. The phenol/Pd molar ratio was kept fixed in all studied cases to establish a fair comparison. These results demonstrated that CNCs behaved like a regular support from a catalytic activity perspective. Good activity obtained with PdNPs@CNCs was also likely enabled by the very small size of the PdNPs. In another work, we could use Pd NPs supported onto CNCs in the enantioselective hydrogenation of prochiral ketones at 4 bars H_2, at room temperature and in water for 2 h (Scheme 1d).[137] Remarkably, here the CNCs not only acted as supports for Pd NPs, but they were actively involved in the reaction, acting as chiral inducers during hydrogenation, to afford enantiomeric excesses (ee) up to 65%. While these are low compared to ees reported for chiral complexes attached to supports, including cellulose,[160] this result is unprecedented for an unmodified biosourced support. Although less active than their Pd counterparts, Ag NPs have proved active for the hydrogenation of aldehydes and have surpassed them in terms of chemoselectivity. For instance, silica-supported Ag NPs were reported for the selective hydrogenation of C=O bonds over C=C bonds.[161,162] Such systems, were the particles are around 5 nm in size were prepared by calcination at 500 °C and proved C=O-selective for citral hydrogenation. In another example, manganese oxide supported AgNPs, produced under strongly acidic conditions (pH = 1), catalyzed the hydrogenation of acetophenone.[163] Polymers, in the form of polyvinylpyrrolidone (PVP), were also used as Ag nanocolloids (4 ± 0.5 nm) supports for the selective reduction of α,β-unsaturated aldehydes.[164] CNCs were used extensively as AgNPs support (see Tables 2 and 3). Our group used them for the reduction of aromatic aldehydes, alkenes and alkynes at 40 bar H_2 and 100 °C for 24 h, with excellent conversions (Scheme 1c).[149] At last, we showed that Ru NPs supported onto CNCs performed remarkably well for the difficult hydrogenation of arenes under very mild conditions (4 bars H_2, room temperature, in water, for 24 h) (Scheme 1e).[138] The product was easily extracted in a biphasic system, and the catalysts could be recycled up to 6 times with no loss of activity.

4.2. Oxidations

Ru NPs supported onto CNFs have been used for catalyzing the oxidation of benzyl alcohol to benzaldehyde at 120 °C for 24 h with 89% yields (Scheme 2).[127] These results proved superior to catalysis done by Ru NPs supported onto titania or alumina. In the proposed mechanism, Ru NPs formed the Ru^{II}=O species with the help of atmospheric oxygen. This is followed by the assistance of formed Ru-oxo species in the formation of benzaldehyde from benzyl alcohol. The system was recyclable up to 4 cycles.

4.3. Coupling reactions

Heck coupling reactions (Scheme 3a) using Pd NPs supported onto nanocelluloses have been studied by various research groups. Our group demonstrated that Heck coupling reaction using model substrates, styrene and iodobenzene, could be carried out efficiently by Pd NPs supported onto CNCs in a 1 : 1 mixture of water–acetonitrile at 100 °C. Using K_2CO_3 as a base, 75% of iodobenzene was converted in stilbene within 24 h, at a molar ratio iodobenzene/Pd of 170/1. Zhou *et al.*

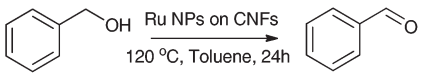

Scheme 2 Oxidation of benzyl alcohol using Ru NPs supported on CNFs as catalysts.

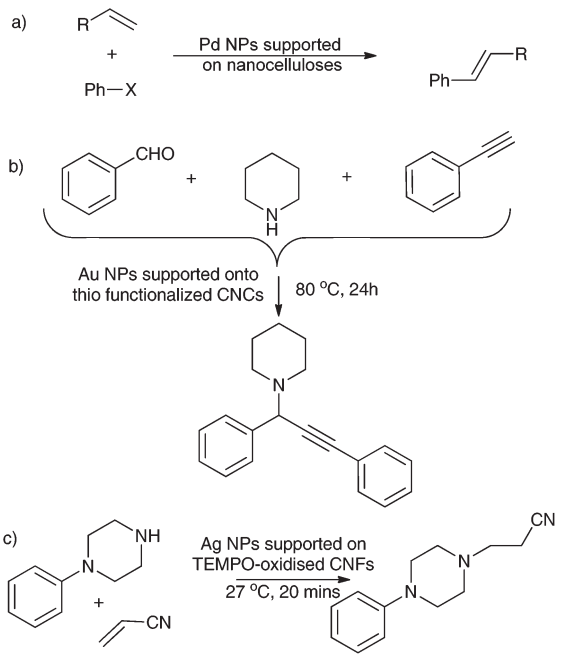

Scheme 3 (a) Heck coupling reaction with Pd NPs supported onto nanocelluloses, (b) A-3 coupling reaction with Au NPs onto CNCs, and (c) aza-Michael reaction with Ag NPs onto CNFs.

carried out a similar Heck coupling reaction in DMF and triethylamine at 120 °C for 10 h, using Pd NPs supported onto bacterial CNFs.[133] They also expanded the scope of the reaction to other aryl halides and acryl acetates. The catalyst was recyclable up to 5 times. In this study, Pd leaching was studied by ICP-AES analysis before and after the fifth cycle. The Pd concentration in the catalyst was found to have dropped. However, no Pd metal was detected in the final coupling product, indicating possible Pd loss during the workup. Thielemans, Walsh and coll. have also used Pd NPs supported onto CNCs for the Heck coupling reactions at 100–130 °C, for 16 h, with good yields.[145] Huang *et al.* carried out an A^3-coupling reaction (coupling of aldehyde–alkyne–amine) utilising Au NPs supported onto thiol-functionalized CNCs (Scheme 3b). The system exhibited excellent activity both in water and without solvent at 80 °C for 24 h, with high promiscuity towards a variety of reactants.[141] The catalyst was recyclable up to 11 cycles. A different study reported the first aza-Michael reaction (Scheme 3c) of 1-phenylpiperazine with acrylonitrile using the Ag NPs supported onto TEMPO-oxidized CNFs at 27 °C, for 20 min with 99% yields and 100% selectivities.[127] This system was recyclable up to 4 cycles.

4.4. Electrocatalysis

Evans *et al.* demonstrated one of the earliest applications for metal NP-nanocellulose hybrid composites in electrolysis in 2003.[125] They used Pd supported onto bacterial CNFs as catalysts for H_2 evolution when incubated with sodium dithionite. This result demonstrated the potential application of bacterial CNFs for anodic oxidation of H_2 and therefore, their aptness in energy conversion devices. Experimental data also showed that bacterial CNFs possessed greater thermal stability and lower H_2 crossover characteristics compared to Nafion 117-based proton exchange membrane (PEM) fuel cells, which are the most prevalent. Another study revealed that Pt NPs supported on bacterial CNFs possessed high electrocatalytic activity in H_2 oxidation reactions.[154] The single cell performance of Pt NPs supported on bacterial CNFs was tested at 20, 30, and 40 °C under non-humidified conditions. In addition, matrix proton conductivity could be improved by doping bacterial CNF pellicles with proton or inorganic acids, increasing the current density. Johnson *et al.* studied Pt NPs supported onto CNCs in electrocatalysis for oxygen electroreduction.[147] Their results were comparable to state-of-the-art Johnson Matthey Pt/C. In another work, they used Ag NPs supported onto CNCs for electrocatalytic oxygen reduction.[142] The electrocatalytic oxygen reduction reaction is a cathode reaction in alkaline fuel cells, and silver is a better cathode material for alkaline fuel cells because it has an activity almost equal to that of platinum but is significantly less expensive.

4.5. Photocatalysis

Photocatalysis provides an efficient way of degrading dyes accumulated in the environment, mainly in water. Metal NP-nanocellulose hybrid composites have been used as photocatalysts for degradation of a model pollutant, methyl orange (MO). CdS supported onto bacterial CNFs demonstrated high-efficiency photocatalysis with 82% MO degradation after 90 min irradiation and recyclability up to 5 times.[152] Similar results were also shown with TiO_2 supported onto bacterial CNFs for degradation of MO.[155] Doping the catalyst with nitrogen enhanced its photocatalytic activity. Notably, both catalysts resulted in better photocatalytic activity than the commercially available ones.

4.6. Biosensing and enzyme immobilisation

Due to their excellent biocompatibility and limited toxicity, metal NP-nanocellulose hybrid composites provide an excellent route for making biosensors and enzyme immobilization. Wang *et al.* developed a high performance biosensor based on Au NP-nanocellulose hybrid composites.[150] Heme proteins such as horseradish peroxidase, hemoglobin and myoglobin were immobilized on the surface of Au NP–bacterial CNF nanocomposites. Heme proteins are important peroxidases that contain iron heme prosthetic groups in their polypeptide pockets, and can catalyze the oxidation of substrates when activated by peroxides. Therefore, to check the bioactivity of these heme proteins, H_2O_2 is often selected as a target compound. The immobilized heme proteins showed electrocatalytic activities towards the reduction of H_2O_2 in the presence of the mediator hydroquinone. The response of the developed biosensor to H_2O_2 was related to the amount of Au NPs in the Au NP-bacterial CNF nanocomposite. In another study, the Au NP-bacterial CNFs were used for the fabrication of a horseradish peroxidase biosensor, which was highly sensitive to H_2O_2 with a detection limit lower than 1 μM.[131] Also, porous composite films containing CNFs and TiO_2 nanoparticles were obtained in a layer-by-layer assembly process for creating conducting pathways for electrons in a relatively open cellulose structure potentially suitable for the immobilization of large redox proteins such as methemoglobin.[124]

Thiol sensors serve as markers for the diagnosis of metabolic diseases like skin lesions, edema, liver damage and pancreatitis. Mac Lachlan and coll. used Au NP-nanocellulose composites for sensing 2-mercaptoethanol.[128] The Au-loaded mesoporous photonic cellulose films exhibited large color changes upon exposure to 2-mercaptoethanol. These results indicated that the mesoporosity of the host matrix renders the NPs accessible to analytes, and alluded to the use of Au NP-loaded mesoporous photonic cellulose for novel sensors.

Luong and coll. used Au NPs supported onto CNCs for the immobilization of enzymes, cyclodextrin glycosyl transferase (CGTase) and alcohol oxidase.[151] This catalytic platform exhibited significant biocatalytic activity with excellent enzyme stability and without apparent loss of the original activity. The recovered specific activities were ~70% and 95% for CGTase and alcohol oxidase, respectively. This strategy provides a novel platform for the scale-up of enzyme-catalyzed processes at the industrial level with improved performance, homogeneity, reusability, and cost effectiveness.

Table 4 Catalytic systems based on nanocelluloses in absence of metal NPs

Catalyst system	Precursor (synthesis of catalyst)	Catalytic reaction	Ref.
Cu-tetrasulfonate PC grafted on CNCs	Phthalocyanine (PC) (electrostatic interaction and H-bonding between cationic CNC and anionic sulfonate Cu-PC)	Aerobic oxidation of alcohols and alkyl arenes	157
Co(II) on ethylenediamine-functionalized CNCs	$CoCl_2$	Oxidation of benzyl alcohols	165
HCl-treated CNFs	—	Chirality-specific hydrolysis of amino-acids	166
HCl-treated CNFs	—	Hydrolysis of esters, monophosphate, amide, and ether bonds: decomposition of coat protein of model viruses	167
Imidazolium-grafted CNCs	—	Ion-exchange reactions	168
Mesoporous α-Fe_2O_3 with CNC support	$FeCl_3$ (sol–gel method)	Photo-degradation of methylene blue	169
Rh(I) on TEMPO-oxidised CNCs	$Rh_2(OOCCF_3)_4$ (ligand exchange)	Cyclopropanation of styrene	156

5. Other types of catalysis

In recent years, a few examples in the literature have emerged where the nanocelluloses have been applied for catalysis without the use of metal NPs. In this section we shall summarize various catalytic systems using nanocelluloses, without metal NPs (Table 4).

Thielemans and coll. modified the surface of CNCs using copper(I) catalyzed azide–alkyne cycloaddition to graft an imidazolium salt (Scheme 4).[168] The modified CNCs were then examined for their potential application in ion-exchange reactions. The ion exchange capability of modified CNCs was tested by suspending them in an aqueous solution of lithium bis(trifluoromethanesulfonyl)imide overnight. The bromide anion was successfully exchanged with bistriflimide. This work demonstrates a method to immobilize imidazolium salts, producing a heterogeneous system in which the anion can be easily exchanged, and hence, provides an opportunity for synthesizing a wide variety of catalytic and ion-exchange systems.

Wada and coll. presented the hydrolytic activities of CNFs through their latest work. They used the abundant nucleophillic hydroxyl groups on the surface of HCl treated-CNFs for hydrolysis of esters, as well as monophosphate, amide, and ether bonds (Scheme 5a).[167] They incubated small organic substrates with CNFs under mild conditions (10 mM HEPES buffer solution, pH 7.4, 30 °C, atmospheric pressure) for examining the hydrolytic activities of CNFs. The order of the hydrolysis rates was estimated to be ester > monophosphate > amide bonds. On the other hand, CNFs could not hydrolyse the ether bonds. The crystalline nanofiber structure of cellulose was essential for their hydrolytic activities. When CNFs obtained from green algae (Cladophora) (which had similar diameters and lengths as those obtained from tunicates) were used under the same reaction conditions, similar activities were observed. This observation suggested that the hydrolytic activities were independent of the crystal polymorphs of CNFs. On the other hand, CNFs obtained from cotton and wood, which have smaller diameters and lengths, showed decreased hydrolytic activities than those from tunicates and green algae, suggesting that the hydrolytic activities were strongly dependent on the cellulose source and their sizes. Following these results, they applied the hydrolytic abilities of CNFs to the decomposition of coat protein of the model virus, filamentous M13 bacteriophage. CNFs could decompose the coat proteins,

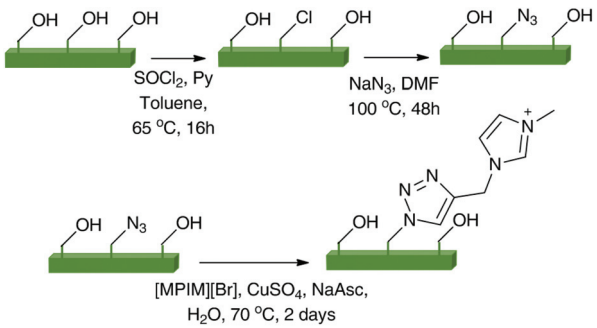

Scheme 4 Surface modification of CNCs.

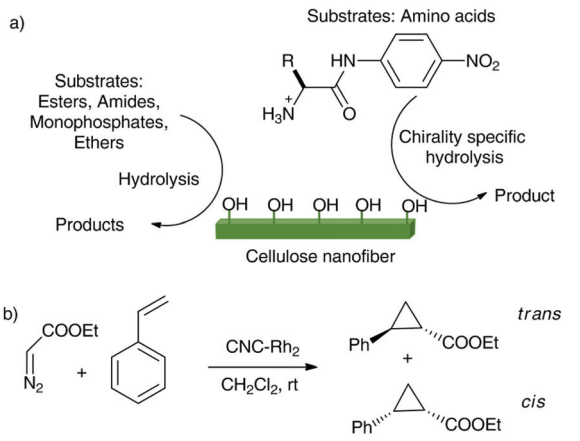

Scheme 5 (a) Hydrolytic activities of HCl-treated CNFs, and (b) cyclopropanation by the heterogeneous catalyst CNC-Rh_2.

followed by a drastic decrease in virus' infection capabilities of host cells. Through their work, they anticipated that the CNFs could lead to a novel class of artificial enzymes and called them cellizymes. In a different study, they used CNFs for chirality-specific hydrolytic activities for model amino acid substrates with activated amide bonds (Scheme 5a).[166] The resulting chiral specificities significantly correlated with the amino acid species and crystal structures of the CNFs.

In an interesting study, Co(II) was immobilised using its coordination to amine-functionalized nanocellulose to obtain a heterogeneous catalyst for the oxidation of various primary and secondary benzylic alcohols to their corresponding aldehydes and ketones, in *o*-xylene at room temperature, with good yields and recyclability.[165] A low loading of Co(II) (1.04 wt%) could be afforded because of distribution of cobalt on the nanocelluloses with high surface area. Another heterogeneous catalyst was devised by grafting copper tetrasulfonate phthalocyanine (Cu-PC) onto CNCs for selective aerobic oxidation of benzylic alcohols to corresponding ketones under mild conditions with good yields.[157] The grafting was due to electrostatic interactions and H-bonding between cationic CNC and anionic sulfonate Cu-PC. The system was recyclable up to 7 times and showed no leaching of Cu during the catalysis. Liang *et al.* synthesized mesoporous α-Fe_2O_3 *via* sol–gel methods using CNCs as template and studied its photocatalytic properties.[169] The prepared α-Fe_2O_3 catalyst was used for the photo degradation of methylene blue, and the results revealed that α-Fe_2O_3 on CNC templates had improved photocatalytic activity than that of samples prepared without CNCs. Liu *et al.* recently designed yet another heterogeneous catalyst using CNCs for cyclopropanation.[156] To prepare the catalyst, the CNCs were synthesized by TEMPO-mediated oxidation of microcrystalline cellulose, transforming the primary hydroxyl groups at C6 position to carboxyl groups. The diRhodium(II) moieties were then anchored on the surface of CNCs by a ligand exchange between $Rh_2(OOCCF_3)_4$ and carboxyl groups to give the CNC-Rh_2 catalyst. Cyclopropanation of styrene with ethyl diazoacetate (Scheme 5b) catalyzed by heterogeneous CNC-Rh_2 catalyst at room temperature gave excellent yields. Remarkably, the study also concluded that the contribution of physisorbed $Rh_2(OOCCF_3)_4$ on CNCs to the reaction was negligible in comparison to its covalently immobilized counterpart.

6. Conclusions

Nanocelluloses, comprising the whole class of crystalline celluloses in the nano-domain (CNCs, CNFs and bacterial CNFs) has proved to be a versatile support for metal NPs. Their high surface area, thermal stability, non-toxicity and inexpensiveness provide researchers a sustainable template for metal NPs. Moreover, the hydroxyl groups on its surface has been utilised in the recent years for reducing metal precursors, and hence, opening a greener approach for metal NP synthesis, without the use of any external reducing agents. The metal NP-nanocellulose hybrid composites have found diverse applications in paper, polymer, plastics, chiral templating, flocculants, aerogels, hydrogels, drug delivery, cosmetics, pharmaceutics and catalysis. This review focused on the use of nanocelluloses for the design of catalytic systems. These demonstrate appealing abilities as recyclable catalysts. Recently, researchers have demonstrated that these nanocelluloses could not only support materials for heterogeneous catalysis, but also play a key role in the reactions themselves, for example as chiral inducers in the enantioselective hydrogenations, or as chiral recognition centres in chirality specific hydrolysis of amino acids. Over the years, the characterisation techniques for these nanocelluloses and their modified hybrids have improved. These advances will heavily steer the catalytic applications of nanocelluloses in the coming years. Nanocellulose suspensions in water provide a robust system in which biphasic catalysis can be explored. These suspensions provide an ionic liquid-like environment to the metal NPs and metal salts in them. Based on that, another noteworthy direction to take would be to investigate the ligand exchange reactions using organometallic precursors in the CNC-water suspension. The system, thus obtained, would be interesting to check for catalysis, for example in C–H activations, C–C coupling reactions, *etc*. We conclude that the use of nanocelluloses in catalytic applications has resulted in the design of exciting novel catalytic systems in the last few years. We expect innovative applications to soon result from these developments.

Acknowledgements

We thank the Natural Science and Engineering Research Council of Canada (NSERC) Discovery Grant program, the Canada Foundation for Innovation (CFI), the Canada Research Chairs (CRC), the Centre for Green Chemistry and Catalysis (CGCC), NSERC-Collaborative Research and Training Experience (CREATE) in Green Chemistry and McGill University for their financial support. We thank Mileeta Kaushik for her contribution to the graphical abstract.

Notes and references

1 M. Kaushik, J.-L. Putaux, C. Fraschini, G. Chauve and A. Moores, Transmission Electron Microscopy for the Characterization of Cellulose Nanocrystals, in *The Transmission Electron Microscope*, Intech, 2015, pp. 129–163.
2 H. Chanzy, *Cellulose*, 2015, 1–4.
3 C. M. Cirtiu, A. F. Dunlop-Brière and A. Moores, *Green Chem.*, 2011, **13**, 288–291.
4 D. Klemm, B. Heublein, H. P. Fink and A. Bohn, *Angew. Chem., Int. Ed.*, 2005, **44**, 3358–3393.
5 K. Benaissi, L. Johnson, D. A. Walsh and W. Thielemans, *Green Chem.*, 2010, **12**, 220–222.

6 X. M. Dong, T. Kimura, J.-F. Revol and D. G. Gray, *Langmuir*, 1996, **12**, 2076–2082.
7 O. van den Berg, J. R. Capadona and C. Weder, *Biomacromolecules*, 2007, **8**, 1353–1357.
8 S. Beck, J. Bouchard and R. Berry, *Biomacromolecules*, 2012, **13**, 1486–1494.
9 E. Lam, S. Hrapovic, E. Majid, J. H. Chong and J. H. T. Luong, *Nanoscale*, 2012, **4**, 997–1002.
10 R. F. Nickerson and J. A. Habrle, *Ind. Eng. Chem. Res.*, 1947, **39**, 1507–1512.
11 B. G. Rånby, *Acta Chem. Scand.*, 1949, **3**, 649–650.
12 B. G. Rånby, *Discuss. Faraday Soc.*, 1951, **11**, 158–164.
13 S. Padalkar, J. R. Capadona, S. J. Rowan, C. Weder, Y.-H. Won, L. A. Stanciu and R. J. Moon, *Langmuir*, 2010, **26**, 8497–8502.
14 I. A. Sacui, R. C. Nieuwendaal, D. J. Burnett, S. J. Stranick, M. Jorfi, C. Weder, E. J. Foster, R. T. Olsson and J. W. Gilman, *ACS Appl. Mater. Interfaces*, 2014, **6**, 6127–6138.
15 S. J. Eichhorn, A. Dufresne, M. Aranguren, N. E. Marcovich, J. R. Capadona, S. J. Rowan, C. Weder, W. Thielemans, M. Roman, S. Renneckar, W. Gindl, S. Veigel, J. Keckes, H. Yano, K. Abe, M. Nogi, A. N. Nakagaito, A. Mangalam, J. Simonsen, A. S. Benight, A. Bismarck, L. A. Berglund and T. Peijs, *J. Mater. Sci.*, 2009, **45**, 1–33.
16 Y. Habibi, L. A. Lucia and O. J. Rojas, *Chem. Rev.*, 2010, **110**, 3479–3500.
17 R. J. Moon, A. Martini, J. Nairn, J. Simonsen and J. Youngblood, *Chem. Soc. Rev.*, 2011, **40**, 3941–3994.
18 N. Lin, J. Huang and A. Dufresne, *Nanoscale*, 2012, **4**, 3274–3294.
19 C. Salas, T. Nypelö, C. Rodriguez-Abreu, C. Carrillo and O. J. Rojas, *Curr. Opin. Colloid Interface Sci.*, 2014, **19**, 383–396.
20 C. Fraschini, G. Chauve, J.-F. L. Berre, S. Ellis, M. Méthot, B. O'Connor and J. Bouchard, *Nord. Pulp Pap. Res. J.*, 2014, **29**, 31–40.
21 B. S. Brito, F. V. Pereira, J.-L. Putaux and B. Jean, *Cellulose*, 2012, **19**, 1527–1536.
22 M. Lopez, H. Bizot, G. Chambat, M.-F. Marais, A. Zykwinska, M.-C. Ralet, H. Driguez and A. Buléon, *Biomacromolecules*, 2010, **11**, 1417–1428.
23 V. Favier, H. Chanzy and J. Cavaille, *Macromolecules*, 1995, **28**, 6365–6367.
24 M. Le Normand, R. Moriana and M. Ek, *Carbohydr. Polym.*, 2014, **111**, 979–987.
25 H. A. Silvério, W. P. F. Neto, N. O. Dantas and D. Pasquini, *Ind. Crops Prod.*, 2013, **44**, 427–436.
26 D. Klemm, F. Kramer, S. Moritz, T. Lindström, M. Ankerfors, D. Gray and A. Dorris, *Angew. Chem., Int. Ed.*, 2011, **50**, 5438–5466.
27 M. Kaushik, W. C. Chen, T. G. M. van de Ven and A. Moores, *Nord. Pulp Pap. Res. J.*, 2014, **29**, 77–81.
28 G. Morandi, L. Heath and W. Thielemans, *Langmuir*, 2009, **25**, 8280–8286.
29 W. Wu and L. Zhang, *Prog. Chem.*, 2014, **26**, 403–414.
30 K. Y. Qiu and A. N. Netravali, *Polym. Rev.*, 2014, **54**, 598–626.
31 N. Lin, J. Huang and A. Dufresne, *Polysaccharide Nanocrystals-Based Materials for Advanced Applications*, Wiley-VCH, Weinheim, 2014.
32 M. Roman, *Ind. Biotechnol.*, 2015, **11**, 25–33.
33 N. Yanamala, M. T. Farcas, M. K. Hatfield, E. R. Kisin, V. E. Kagan, C. L. Geraci and A. A. Shvedova, *ACS Sustainable Chem. Eng.*, 2014, **2**, 1691–1698.
34 K. Kümmerer, J. Menz, T. Schubert and W. Thielemans, *Chemosphere*, 2011, **82**, 1387–1392.
35 T. Kovacs, V. Naish, B. O'Connor, C. Blaise, F. Gagné, L. Hall, V. Trudeau and P. Martel, *Nanotoxicology*, 2010, **4**, 255–270.
36 Celluforce, http://celluforce.com/en/, (accessed 29 March 2015, 2015).
37 R. H. Marchessault, F. F. Morehead and N. M. Walter, *Nature*, 1959, **184**, 632–633.
38 J.-F. Revol, L. Godbout, X.-M. Dong, D. G. Gray, H. Chanzy and G. Maret, *Liq. Cryst.*, 1994, **16**, 127–134.
39 J. F. Revol, H. Bradford, J. Giasson, R. H. Marchessault and D. G. Gray, *Int. J. Biol. Macromol.*, 1992, **14**, 170–172.
40 K. E. Shopsowitz, H. Qi, W. Y. Hamad and M. J. MacLachlan, *Nature*, 2010, **468**, 422–425.
41 J. A. Kelly, K. E. Shopsowitz, J. M. Ahn, W. Y. Hamad and M. J. MacLachlan, *Langmuir*, 2012, **28**, 17256–17262.
42 K. E. Shopsowitz, J. A. Kelly, W. Y. Hamad and M. J. MacLachlan, *Adv. Funct. Mater.*, 2014, **24**, 327–338.
43 H. Qi, K. E. Shopsowitz, W. Y. Hamad and M. J. MacLachlan, *J. Am. Chem. Soc.*, 2011, **133**, 3728–3731.
44 K. E. Shopsowitz, W. Y. Hamad and M. J. MacLachlan, *Angew. Chem., Int. Ed.*, 2011, **50**, 10991–10995.
45 D. Zhang and L. Qi, *Chem. Commun.*, 2005, 2735–2737.
46 Y. Shin and G. J. Exarhos, *Mater. Lett.*, 2007, **61**, 2594–2597.
47 A. Ivanova, D. Fattakhova-Rohlfing, B. E. Kayaalp, J. Rathouský and T. Bein, *J. Am. Chem. Soc.*, 2014, **136**, 5930–5937.
48 A. Querejeta-Fernández, G. Chauve, M. Methot, J. Bouchard and E. Kumacheva, *J. Am. Chem. Soc.*, 2014, **136**, 4788–4793.
49 M. G. Campbell, Q. Liu, A. Sanders, J. S. Evans and I. I. Smalyukh, *Materials*, 2014, **7**, 3021–3033.
50 V. Favier, G. Canova, J. Cavaillé, H. Chanzy, A. Dufresne and C. Gauthier, *Polym. Adv. Technol.*, 1995, **6**, 351–355.
51 A. Dufresne, *Can. J. Chem.*, 2008, **86**, 484–494.
52 J. Yang, C.-R. Han, J.-F. Duan, M.-G. Ma, X.-M. Zhang, F. Xu, R.-C. Sun and X.-M. Xie, *J. Mater. Chem.*, 2012, **22**, 22467–22480.
53 X. Yang and E. D. Cranston, *Chem. Mater.*, 2014, **26**, 6016–6025.
54 H. Dong, J. F. Snyder, D. T. Tran and J. L. Leadore, *Carbohydr. Polym.*, 2013, **95**, 760–767.
55 Y. Liu, Y. Li, G. Yang, X. Zheng and S. Zhou, *ACS Appl. Mater. Interfaces*, 2015, **7**, 4118–4126.

56 S. Eyley, S. Shariki, S. E. C. Dale, S. Bending, F. Marken and W. Thielemans, *Langmuir*, 2012, **28**, 6514–6519.
57 K. H. M. Kan, J. Li, K. Wijesekera and E. D. Cranston, *Biomacromolecules*, 2013, **14**, 3130–3139.
58 S. Eyley, D. Vandamme, S. Lama, G. Van den Mooter, K. Muylaert and W. Thielemans, *Nanoscale*, 2015, **7**, 14413–14421.
59 M. Jorfi and E. J. Foster, *J. Appl. Polym. Sci.*, 2015, **132**, 41719–41738.
60 V. Incani, C. Danumah and Y. Boluk, *Cellulose*, 2013, **20**, 191–200.
61 A. Isogai, *J. Wood Sci.*, 2013, **59**, 449–459.
62 M. Giese, L. K. Blusch, M. K. Khan and M. J. MacLachlan, *Angew. Chem., Int. Ed.*, 2015, **54**, 2888–2910.
63 H. Wei, K. Rodriguez, S. Renneckar and P. J. Vikesland, *Environ. Sci.: Nano*, 2014, **1**, 302–316.
64 J. Huang, P. R. Chang and A. Dufresne, *Polysaccharide Nanocrystals: Current Status and Prospects in Material Science*, Wiley-VCH, Weinheim, 2014.
65 F. Hu, S. Fu, J. Huang, D. P. Anderson and P. R. Chang, *Structure and Properties of Polysaccharide Nanocrystals*, Wiley-VCH, Weinheim, 2014.
66 Y. Habibi, *Chem. Soc. Rev.*, 2014, **43**, 1519–1542.
67 S. Eyley and W. Thielemans, *Nanoscale*, 2014, **6**, 7764–7779.
68 K. Missoum, M. N. Belgacem and J. Bras, *Materials*, 2013, **6**, 1745–1766.
69 E. Lam, K. B. Male, J. H. Chong, A. C. W. Leung and J. H. T. Luong, *Trends Biotechnol.*, 2012, **30**, 283–290.
70 H. Khalil, A. H. Bhat and A. F. I. Yusra, *Carbohydr. Polym.*, 2012, **87**, 963–979.
71 E. C. Ramires and A. Dufresne, *Tappi J.*, 2011, **10**, 9–16.
72 S. J. Eichhorn, *Soft Matter*, 2011, **7**, 303–315.
73 P. Lu and Y.-L. Hsieh, *Carbohydr. Polym.*, 2010, **82**, 329–336.
74 M. A. S. Azizi Samir, F. Alloin and A. Dufresne, *Biomacromolecules*, 2005, **6**, 612–626.
75 H. Charreau, M. L. Foresti and A. Vazquez, *Recent Pat. Nanotechnol.*, 2013, **7**, 56–80.
76 D. J. Cole-Hamilton and R. Tooze, *Catalyst Separation, Recovery and Recycling*, Springer, Dordrecht, The Netherlands, 2006.
77 D. J. Cole-Hamilton, *Science*, 2003, **299**, 1702–1706.
78 J. Dupont, G. S. Fonseca, A. P. Umpierre, P. F. Fichtner and S. R. Teixeira, *J. Am. Chem. Soc.*, 2002, **124**, 4228–4229.
79 Technical Association of Pulp and Paper Industries (TAPPI), http://www.tappi.org.
80 L. Heux, G. Chauve and C. Bonini, *Compos. Interfaces*, 2000, **16**, 8210–8212.
81 S. Elazzouzi-Hafraoui, Y. Nishiyama, J.-L. Putaux, L. Heux, F. Dubreuil and C. Rochas, *Biomacromolecules*, 2008, **9**, 57–65.
82 P. Lu and Y.-L. Hsieh, *Carbohydr. Polym.*, 2012, **87**, 564–573.
83 N. Johar, I. Ahmad and A. Dufresne, *Ind. Crops Prod.*, 2012, **37**, 93–99.
84 M. S. Peresin, Y. Habibi, J. O. Zoppe, J. J. Pawlak and O. J. Rojas, *Biomacromolecules*, 2010, **11**, 674–681.
85 Y. Habibi, A.-L. Goffin, N. Schiltz, E. Duquesne, P. Dubois and A. Dufresne, *J. Mater. Chem.*, 2008, **18**, 5002–5010.
86 A. Junior de Menezes, G. Siqueira, A. A. S. Curvelo and A. Dufresne, *Polymer*, 2009, **50**, 4552–4563.
87 N. L. Garcia de Rodriguez, W. Thielemans and A. Dufresne, *Cellulose*, 2006, **13**, 261–270.
88 N. Duran, A. Paula Lemes and A. B. Seabra, *Recent Pat. Nanotechnol.*, 2012, **6**, 16–28.
89 J. Araki, M. Wada, S. Kuga and T. Okano, *J. Wood Sci.*, 1999, **45**, 258–261.
90 D. Bondeson, A. Mathew and K. Oksman, *Cellulose*, 2006, **13**, 171–180.
91 R. J. M. M. T. Postek, A. W. Rudie and M. A. Bilodeau, *Production and Applications of Cellulose Nanomaterials*, Technical Association of Pulp and Paper Industry, TAPPI, Peachtree Corners, GA, August 01, 2013.
92 J. R. Capadona, K. Shanmuganathan, S. Trittschuh, S. Seidel, S. J. Rowan and C. Weder, *Biomacromolecules*, 2009, **10**, 712–716.
93 F. Kimura, T. Kimura, M. Tamura, A. Hirai, M. Ikuno and F. Horii, *Langmuir*, 2005, **21**, 2034–2037.
94 M. N. Anglès and A. Dufresne, *Macromolecules*, 2000, **33**, 8344–8353.
95 M. Roman and W. T. Winter, *Biomacromolecules*, 2004, **5**, 1671–1677.
96 M. Grunert and W. T. Winter, *J. Polym. Environ.*, 2002, **10**, 27–30.
97 J. Araki and S. Kuga, *Langmuir*, 2001, **17**, 4493–4496.
98 D. Astruc, *Nanoparticles and Catalysis*, Wiley-VCH, Weinheim, 2008.
99 Z. Shi, J. Tang, L. Chen, C. Yan, S. Tanvir, W. A. Anderson, R. M. Berry and K. C. Tam, *J. Mater. Chem. B*, 2015, **3**, 603–611.
100 F. Hoeng, A. Denneulin, C. Neuman and J. Bras, *J. Nanopart. Res.*, 2015, **17**, 1–14.
101 A. R. Lokanathan, K. M. A. Uddin, O. J. Rojas and J. Laine, *Biomacromolecules*, 2014, **15**, 373–379.
102 M. S. Wang, F. Jiang, Y. L. Hsieh and N. Nitin, *J. Mater. Chem. B*, 2014, **2**, 6226–6235.
103 R. Xiong, C. Lu, W. Zhang, Z. Zhou and X. Zhang, *Carbohydr. Polym.*, 2013, **95**, 214–219.
104 G. Yang, J. Xie, F. Hong, Z. Cao and X. Yang, *Carbohydr. Polym.*, 2012, **87**, 839–845.
105 G. Yang, J. Xie, Y. Deng, Y. Bian and F. Hong, *Carbohydr. Polym.*, 2012, **87**, 2482–2487.
106 H. Liu, J. Song, S. Shang, Z. Song and D. Wang, *ACS Appl. Mater. Interfaces*, 2012, **4**, 2413–2419.
107 H. Liu, D. Wang, Z. Song and S. Shang, *Cellulose*, 2011, **18**, 67–74.
108 N. Drogat, R. Granet, V. Sol, A. Memmi, N. Saad, C. Klein Koerkamp, P. Bressollier and P. Krausz, *J. Nanopart. Res.*, 2011, **13**, 1557–1562.
109 I. Diez, P. Eronen, M. Osterberg, M. B. Linder, O. Ikkala and R. H. Ras, *Macromol. Biosci.*, 2011, **11**, 1185–1191.

110 H. S. Barud, T. Regiani, R. F. Marques, W. R. Lustri, Y. Messaddeq and S. J. Ribeiro, *J. Nanomater.*, 2011, **2011**, 1–10.
111 L. Maria, A. L. Santos, P. C. Oliveira, A. S. Valle, H. S. Barud, Y. Messaddeq and S. J. Ribeiro, *Polimeros*, 2010, **20**, 72–77.
112 S. Ifuku, M. Tsuji, M. Morimoto, H. Saimoto and H. Yano, *Biomacromolecules*, 2009, **10**, 2714–2717.
113 P. A. Marques, H. I. Nogueira, R. J. Pinto, C. P. Neto and T. Trindade, *J. Raman Spectrosc.*, 2008, **39**, 439–443.
114 W. Hu, S. Chen, X. Li, S. Shi, W. Shen, X. Zhang and H. Wang, *Mater. Sci. Eng., C*, 2009, **29**, 1216–1219.
115 Y. Shin, I.-T. Bae, B. W. Arey and G. J. Exarhos, *J. Phys. Chem. C*, 2008, **112**, 4844–4848.
116 S. Azizi, M. B. Ahmad, M. Z. Hussein and N. A. Ibrahim, *Molecules*, 2013, **18**, 6269–6280.
117 R. J. Pinto, P. A. Marques, M. A. Martins, C. P. Neto and T. Trindade, *J. Colloid Interface Sci.*, 2007, **312**, 506–512.
118 X. Li, S. Chen, W. Hu, S. Shi, W. Shen, X. Zhang and H. Wang, *Carbohydr. Polym.*, 2009, **76**, 509–512.
119 C. Tian, S. Fu and L. A. Lucia, *Cellulose*, 2015, **22**, 1–17.
120 L. Chen, R. M. Berry and K. C. Tam, *ACS Sustainable Chem. Eng.*, 2015, **2**, 951–958.
121 Y. Shin, I.-T. Bae, B. W. Arey and G. J. Exarhos, *Mater. Lett.*, 2007, **61**, 3215–3217.
122 Y. Shin, J. M. Blackwood, I.-T. Bae, B. W. Arey and G. J. Exarhos, *Mater. Lett.*, 2007, **61**, 4297–4300.
123 C. Schütz, J. Sort, Z. Bacsik, V. Oliynyk, E. Pellicer, A. Fall, L. Wågberg, L. Berglund, L. Bergström and G. Salazar-Alvarez, *PLoS One*, 2012, **7**, 45828–45834.
124 M. J. Bonné, E. V. Milsom, M. Helton, W. Thielemans, S. Wilkins and F. Marken, *Electrochem. Commun.*, 2007, **9**, 1985–1990.
125 B. R. Evans, H. M. O'Neill, V. P. Malyvanh, I. Lee and J. Woodward, *Biosens. Bioelectron.*, 2003, **18**, 917–923.
126 B. Ramaraju, T. Imae and A. G. Destaye, *Appl. Catal., A*, 2015, **492**, 184–189.
127 M. Gopiraman, H. Bang, G. Yuan, C. Yin, K.-H. Song, J. S. Lee, I. M. Chung, R. Karvembu and I. S. Kim, *Carbohydr. Polym.*, 2015, **132**, 554–564.
128 M. Schlesinger, M. Giese, L. K. Blusch, W. Y. Hamad and M. J. MacLachlan, *Chem. Commun.*, 2015, **51**, 530–533.
129 O. Eisenhut and E. Kuhn, *Angew. Chem.*, 1942, **55**, 198–206.
130 H. Koga, E. Tokunaga, M. Hidaka, Y. Umemura, T. Saito, A. Isogai and T. Kitaoka, *Chem. Commun.*, 2010, **46**, 8567–8569.
131 T. Zhang, W. Wang, D. Zhang, X. Zhang, Y. Ma, Y. Zhou and L. Qi, *Adv. Funct. Mater.*, 2010, **20**, 1152–1160.
132 W. Wang, H. Y. Li, D. W. Zhang, J. Jiang, Y. R. Cui, S. Qiu, Y. L. Zhou and X. X. Zhang, *Electroanalysis*, 2010, **22**, 2543–2550.
133 P. Zhou, H. Wang, J. Yang, J. Tang, D. Sun and W. Tang, *Ind. Eng. Chem. Res.*, 2012, **51**, 5743–5748.
134 Z. H. Zhou, C. H. Lu, X. D. Wu and X. X. Zhang, *RSC Adv.*, 2013, **3**, 26066–26073.
135 A. Azetsu, H. Koga, A. Isogai and T. Kitaoka, *Catalyst*, 2011, **1**, 83–96.
136 D. Sun, J. Yang, J. Li, J. Yu, X. Xu and X. Yang, *Appl. Surf. Sci.*, 2010, **256**, 2241–2244.
137 M. Kaushik, K. Basu, C. Benoit, C. M. Cirtiu, H. Vali and A. Moores, *J. Am. Chem. Soc.*, 2015, **137**, 6124–6127.
138 M. Kaushik, H. M. Friedman, M. Bateman and A. Moores, *RSC Adv.*, 2015, **5**, 53207–53210.
139 J. Tang, Z. Shi, R. M. Berry and K. C. Tam, *Ind. Eng. Chem. Res.*, 2015, **54**, 3299–3308.
140 L. Chen, W. Cao, P. J. Quinlan, R. M. Berry and K. C. Tam, *ACS Sustainable Chem. Eng.*, 2015, **3**, 978–985.
141 J.-L. Huang, D. G. Gray and C.-J. Li, *Beilstein J. Org. Chem.*, 2013, **9**, 1388–1396.
142 L. Johnson, W. Thielemans and D. A. Walsh, *J. Mater. Chem.*, 2010, **20**, 1737–1743.
143 X. D. Wu, C. H. Lu, Z. H. Zhou, G. P. Yuan, R. Xiong and X. X. Zhang, *Environ. Sci.: Nano*, 2014, **1**, 71–79.
144 X. Wu, C. Lu, W. Zhang, G. Yuan, R. Xiong and X. Zhang, *J. Mater. Chem. A*, 2013, **1**, 8645–8652.
145 M. Rezayat, R. K. Blundell, J. E. Camp, D. A. Walsh and W. Thielemans, *ACS Sustainable Chem. Eng.*, 2014, **2**, 1241–1250.
146 X. B. Lin, M. Wu, D. Y. Wu, S. Kuga, T. Endo and Y. Huang, *Green Chem.*, 2011, **13**, 283–287.
147 L. Johnson, W. Thielemans and D. A. Walsh, *Green Chem.*, 2011, **13**, 1686–1693.
148 P. Dhar, A. Kumar and V. Katiyar, *Cellulose*, 2015, 1–17.
149 M. Kaushik, A. Y. Li, R. Hudson, M. Masnadi, C.-J. Li and A. Moores, *Green Chem.*, 2016, **18**, 129–133.
150 W. Wang, T. J. Zhang, D. W. Zhang, H. Y. Li, Y. R. Ma, L. M. Qi, Y. L. Zhou and X. X. Zhang, *Talanta*, 2011, **84**, 71–77.
151 K. A. Mahmoud, K. B. Male, S. Hrapovic and J. H. T. Luong, *ACS Appl. Mater. Interfaces*, 2009, **1**, 1383–1386.
152 J. Yang, J. Yu, J. Fan, D. Sun, W. Tang and X. Yang, *J. Hazard. Mater.*, 2011, **189**, 377–383.
153 R. Bendi and T. Imae, *RSC Adv.*, 2013, **3**, 16279–16282.
154 J. Yang, D. Sun, J. Li, X. Yang, J. Yu, Q. Hao, W. Liu, J. Liu, Z. Zou and J. Gu, *Electrochim. Acta*, 2009, **54**, 6300–6305.
155 D. Sun, J. Yang and X. Wang, *Nanoscale*, 2010, **2**, 287–292.
156 J. Liu, A. Plog, P. Groszewicz, L. Zhao, Y. Xu, H. Breitzke, A. Stark, R. Hoffmann, T. Gutmann and K. Zhang, *Chem. – Eur. J.*, 2015, **21**, 12414–12420.
157 P. Chauhan and N. Yan, *RSC Adv.*, 2015, **5**, 37517–37520.
158 D. Astruc, F. Lu and J. R. Aranzaes, *Angew. Chem., Int. Ed.*, 2005, **44**, 7852–7872.
159 J. G. de Vries and C. J. Elsevier, *Handbook of Homogeneous Hydrogenation*, Wiley-VCH, Weinheim, 2007.
160 T. Yasukawa, H. Miyamura and S. Kobayashi, *Chem. Sci.*, 2015, **6**, 6224–6229.
161 P. Claus, *Top. Catal.*, 1998, **5**, 51–62.
162 M. Steffan, A. Jakob, P. Claus and H. Lang, *Catal. Commun.*, 2009, **10**, 437–441.

163 G. D. Yadav and R. K. Mewada, *Catal. Today*, 2012, **198**, 330–337.
164 P. G. Mertens, F. Cuypers, P. Vandezande, X. Ye, F. Verpoort, I. F. Vankelecom and D. E. De Vos, *Appl. Catal., A*, 2007, **325**, 130–139.
165 A. Shaabani, S. Keshipour, M. Hamidzad and M. Seyyedhamzeh, *J. Chem. Sci.*, 2014, **126**, 111–115.
166 T. Serizawa, T. Sawada and M. Wada, *Chem. Commun.*, 2013, **49**, 8827–8829.
167 T. Serizawa, T. Sawada, H. Okura and M. Wada, *Biomacromolecules*, 2013, **14**, 613–617.
168 S. Eyley and W. Thielemans, *Chem. Commun.*, 2011, **47**, 4177–4179.
169 H. Liang, K. Liu and Y. Ni, *Mater. Lett.*, 2015, **159**, 218–220.